Chemistry–A European Journal

Supporting Information

New Photosensitizers Based on Heteroleptic Cu^{I} Complexes and CO_2 Photocatalytic Reduction with $[Ni^{II}(cyclam)]Cl_2$

Lisa-Lou Gracia,[a] Luisa Luci,[a, b] Cecilia Bruschi,[a] Letizia Sambri,[b] Patrick Weis,[c] Olaf Fuhr,[d] and Claudia Bizzarri*[a]

Author Contributions

C.B. Conceptualization: Lead; Data curation: Lead; Formal analysis: Supporting; Funding acquisition: Lead; Investigation: Lead; Project administration: Lead; Resources: Lead; Supervision: Lead; Validation: Lead; Writing - Original Draft: Lead; Writing - Review & Editing: Lead
L.G. Data curation: Supporting; Formal analysis: Lead; Investigation: Supporting; Writing - Review & Editing: Equal; experimental analysis and synthesis: Lead
L.L. Data curation: Supporting; Formal analysis: Supporting; synthesis: Equal
C.B. Data curation: Supporting; Formal analysis: Supporting; Investigation: Supporting; Writing - Review & Editing: Supporting; photophysical investigation: Equal
L.S. Project administration: Supporting; Supervision: Supporting; Writing - Review & Editing: Supporting
P.W. Writing - Review & Editing: Supporting; Mass Analysis: Lead
O.F. Writing - Review & Editing: Supporting; Crystallographic Analysis: Lead.

Table of contents

1. ^{1}H, ^{13}C NMR of 1, 2a, 2b and 2c

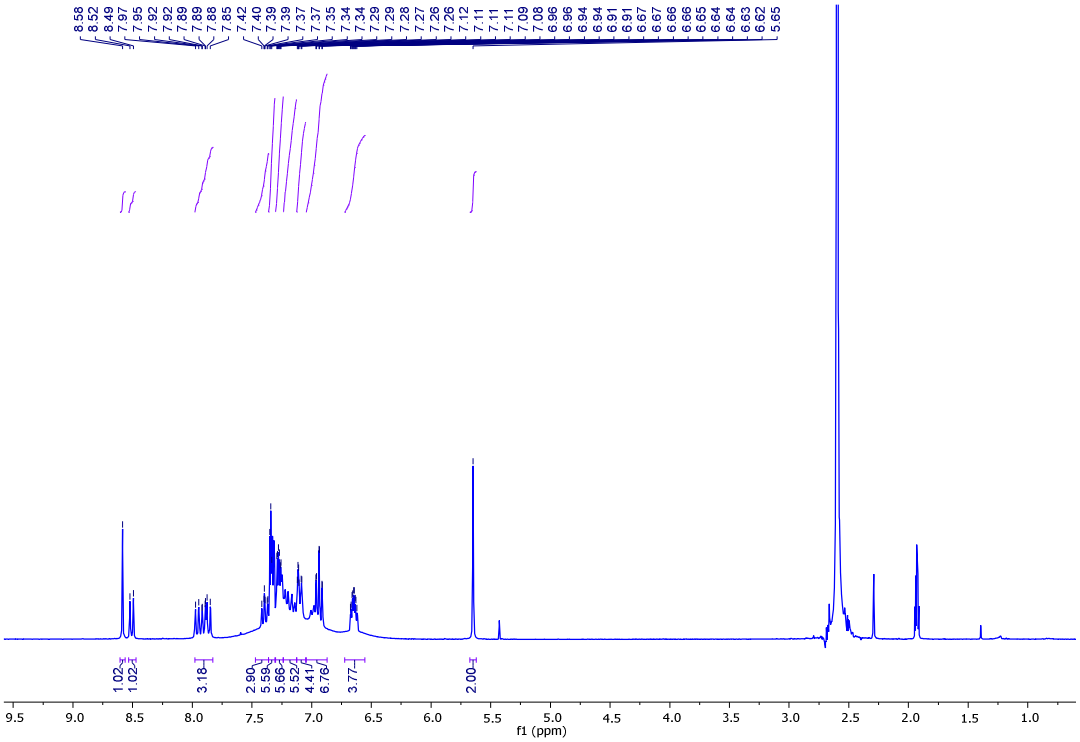

Figure S1. ^{1}H NMR (300 MHz) of **1** in d3-acetonitrile (residual solvent peaks: 2.19ppm (water); 1.90 ppm (CH_3CN))

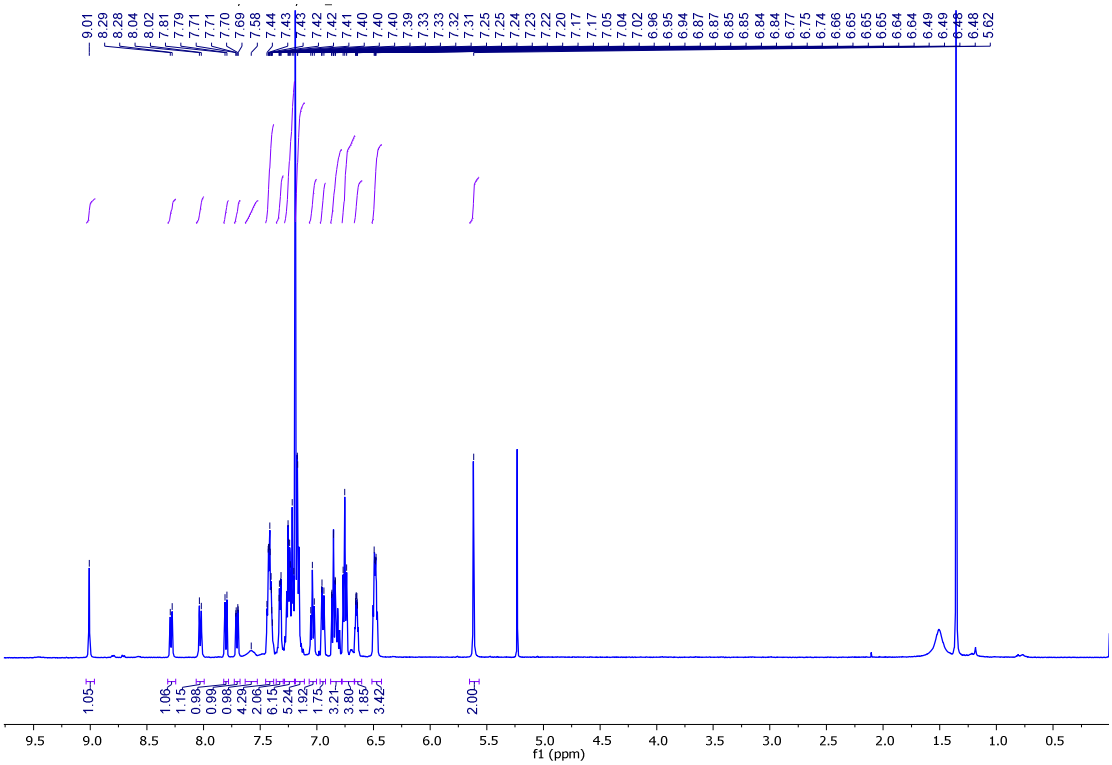

Figure S2. ^{1}H NMR (300 MHz) of **1** in $CDCl_3$ (residual solvent peaks: 7.26 ppm ($CHCl_3$); 5.33 ppm (CH_2Cl_2); 1.50 ppm(water); 1.43 ppm (C_6H_{12})).

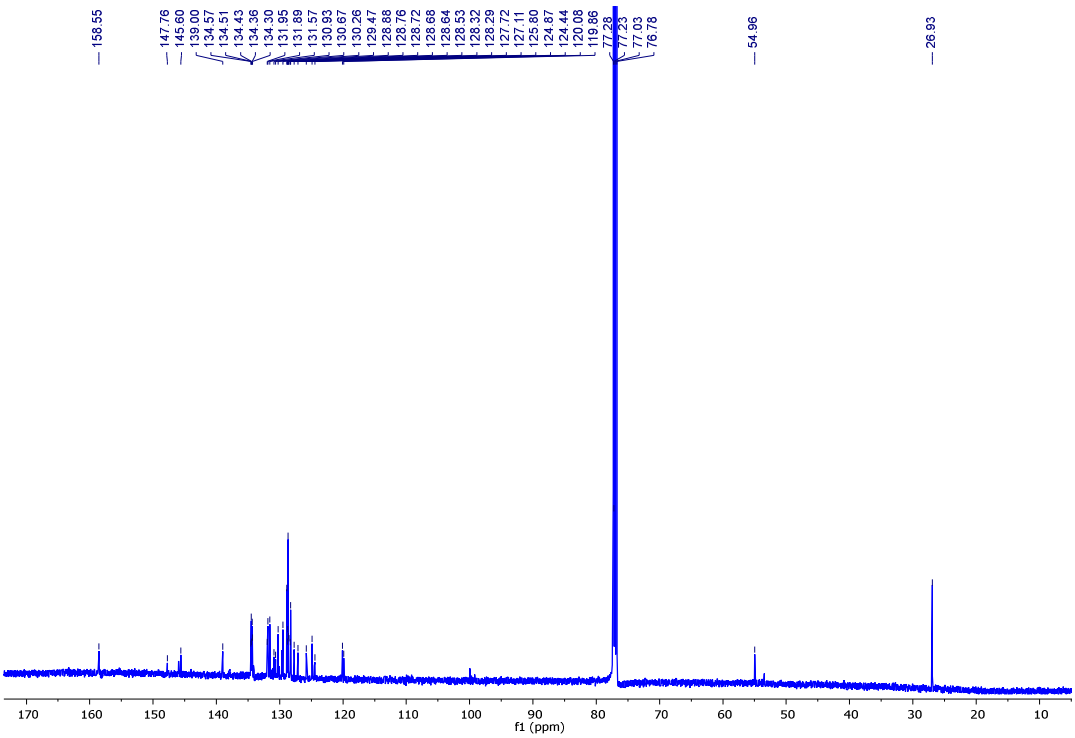

Figure S3. ^{13}C NMR (300 MHz) of **1** in $CDCl_3$ (residual solvent peaks: 77.16 ppm ($CHCl_3$); 53.52 ppm (CH_2Cl_2); 26.94 ppm (C_6H_{12})).

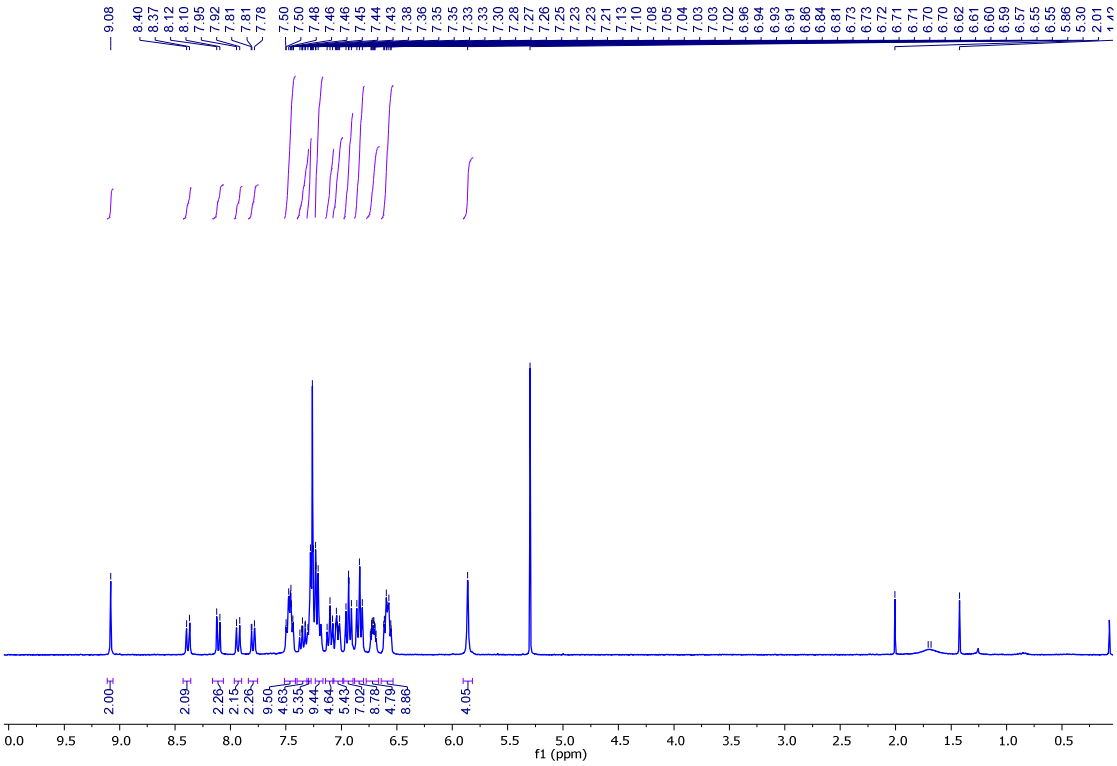

Figure S4. ^{1}H NMR (300 MHz) of **2a** in $CDCl_3$ (residual solvent peaks: 7.26 ppm ($CHCl_3$); 5.33 ppm (CH_2Cl_2); 2.10 (CH_3CN) 1.50 ppm (water); 1.43 ppm (C_6H_{12})).

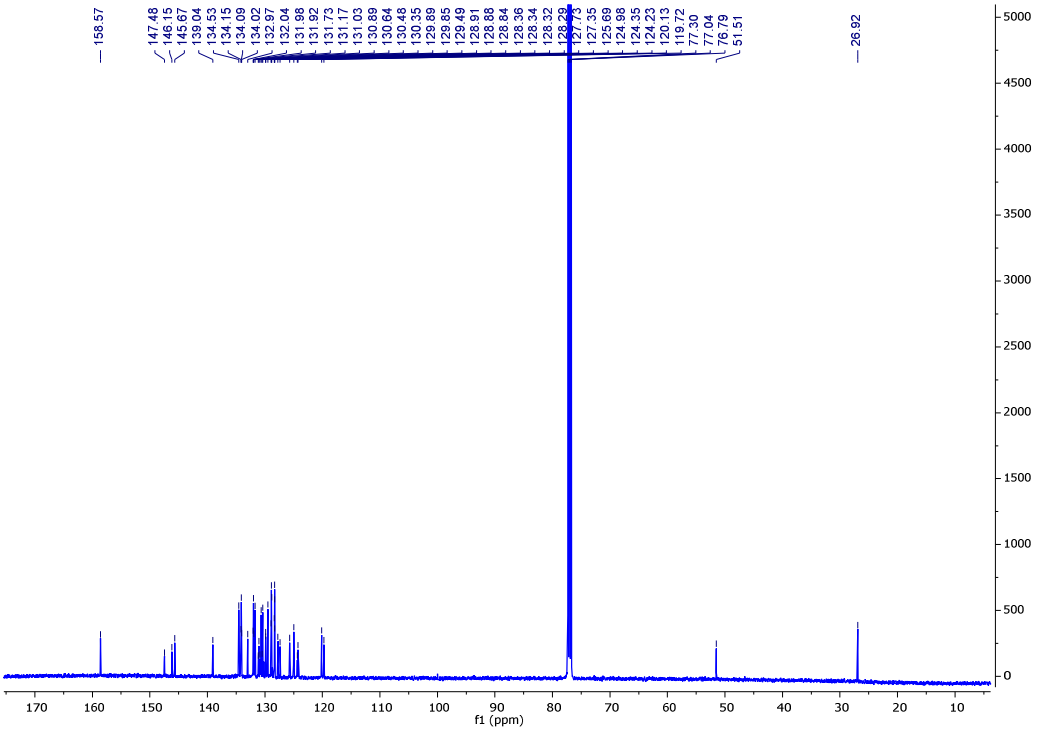

Figure S5. ^{13}C NMR (125 MHz) of **2a** in $CDCl_3$ (residual solvent peaks: 77.16 ppm ($CHCl_3$); 26.94 ppm (C_6H_{12})).

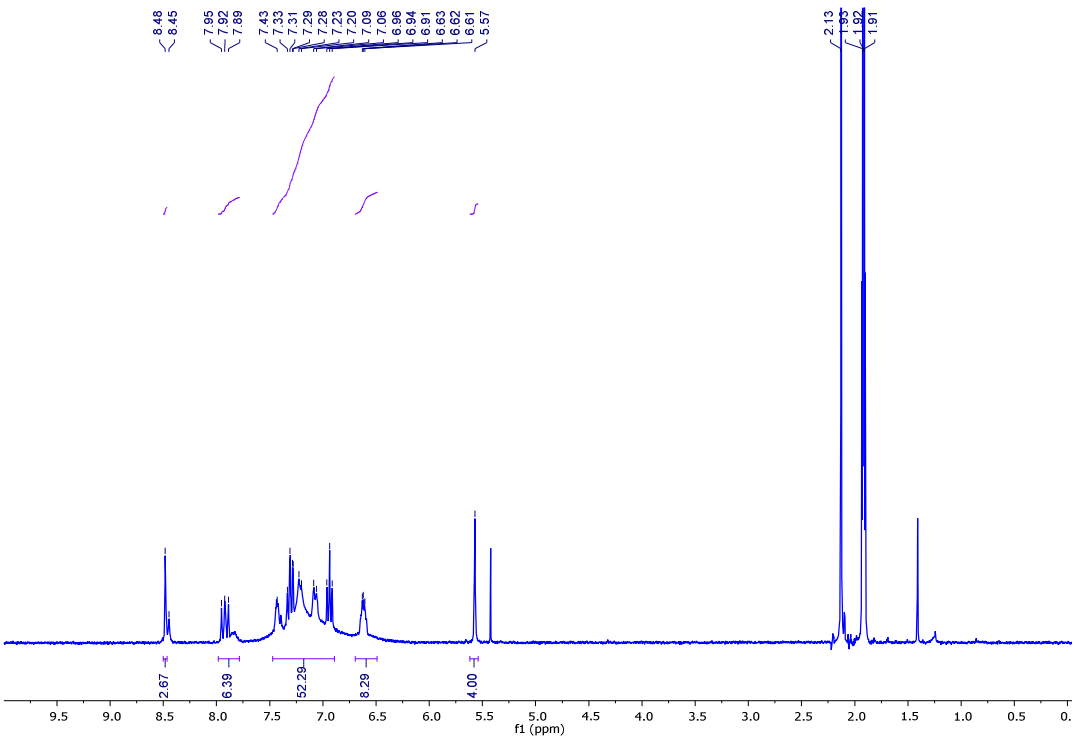

Figure S6. ^{1}H NMR (300 MHz) of **2b** in d3-acetonitrile (residual solvent peaks: 5.47 (CH_2Cl_2); 2.19ppm (water); 1.90 ppm)

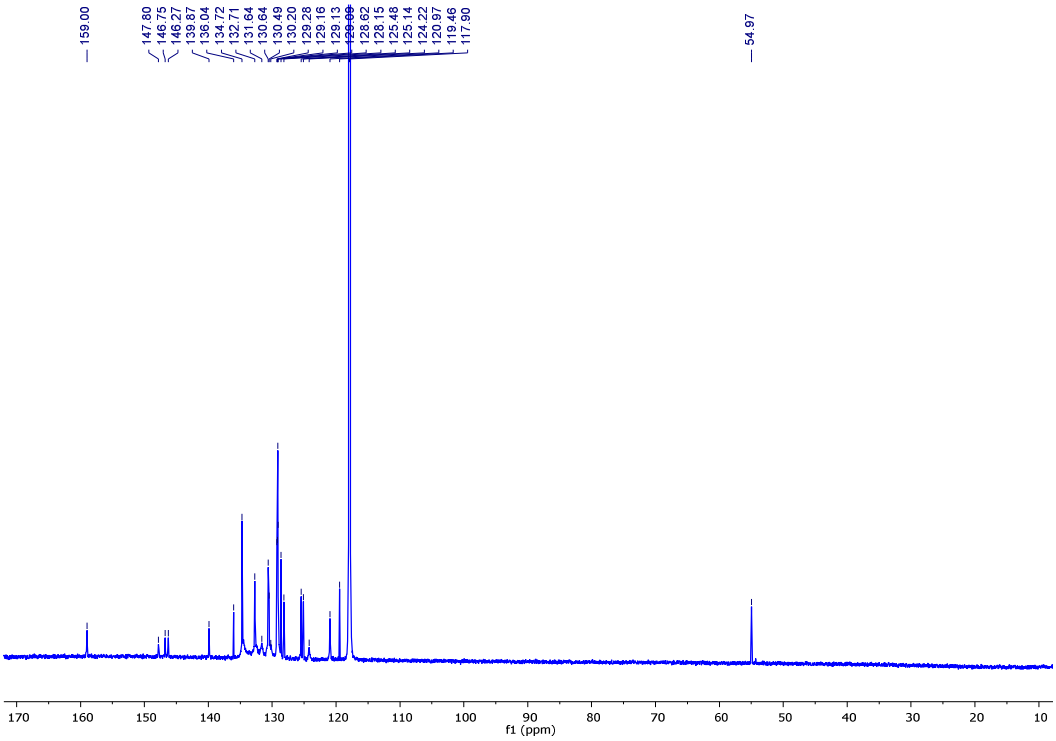

Figure S7. ^{13}C NMR (126 MHz) of **2b** in d3-acetonitrile (solvent peaks: 118.26 ppm, 1.79 ppm).

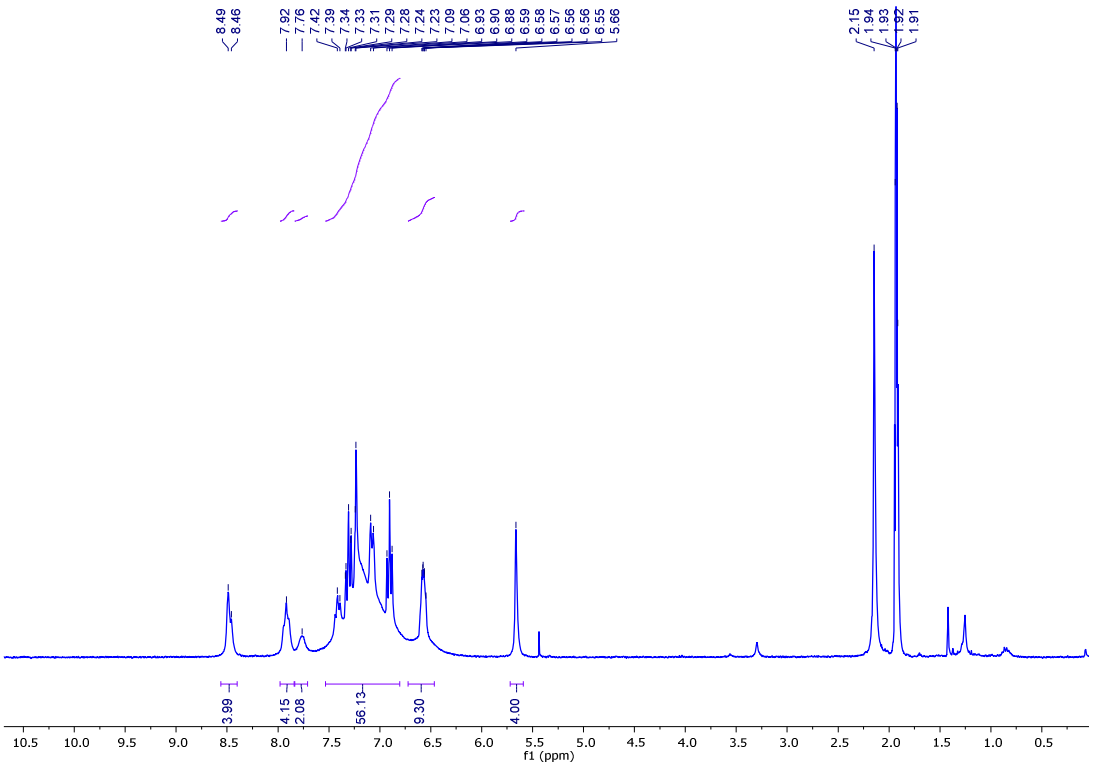

Figure S8. ^{1}H NMR (300 MHz) of **2c** in d3-acetonitrile (residual solvent peaks: 5.45 (CH_2Cl_2); 2.19ppm (water); 1.90 ppm (CH_3CN))

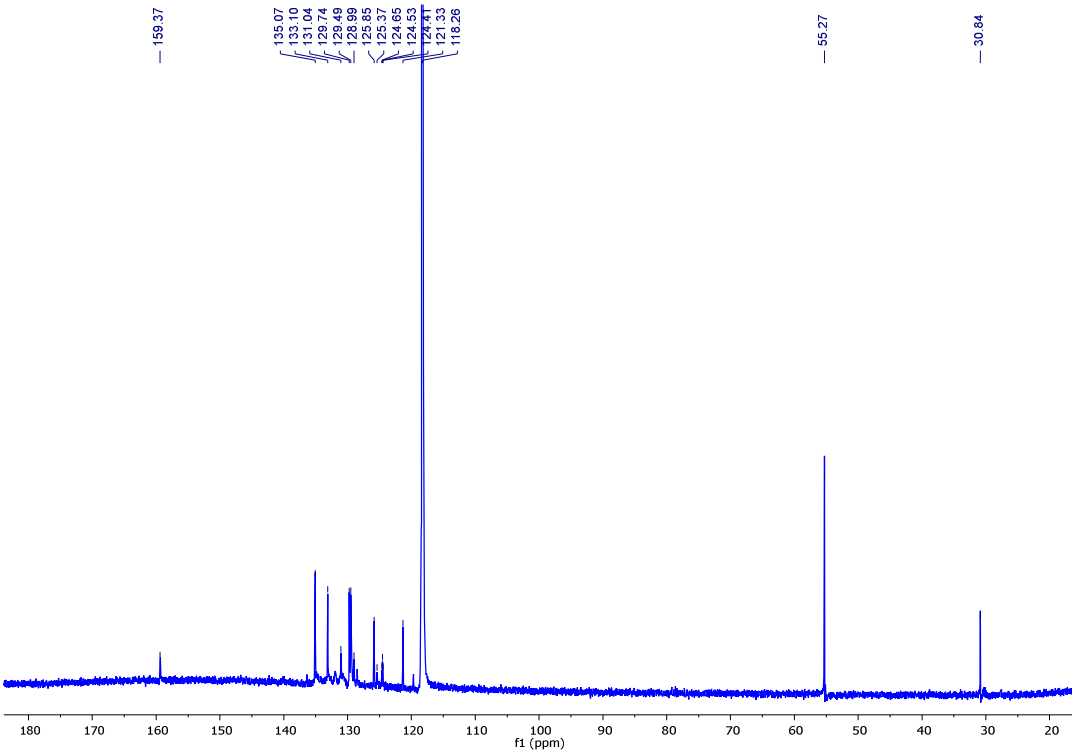

Figure S9. ^{13}C NMR (126 MHz) of **2b** in d3-acetonitrile (solvent peaks: 118.26 ppm, 1.79 ppm; 31.26 (grease)).

2. ^{1}H NMR Stability test of 1, 2a, 2b and 2c in CD_3CN

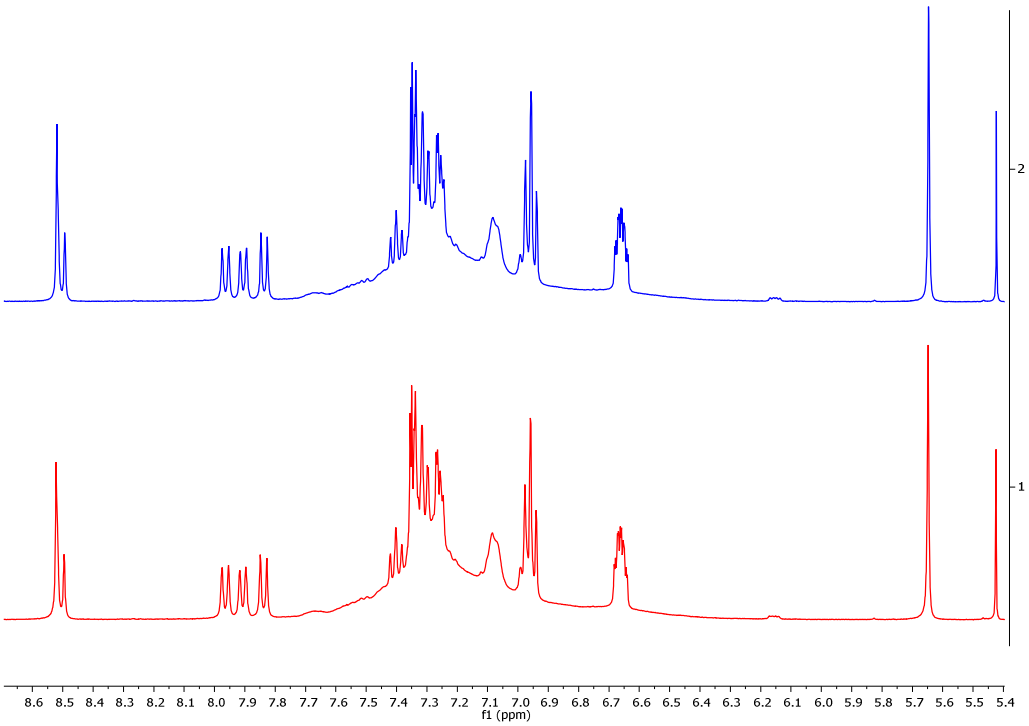

Figure S10. Stability test in d3-acetonitrile of **1**. ^{1}H NMR (300MHz) recorded on the same probe after 1 week.

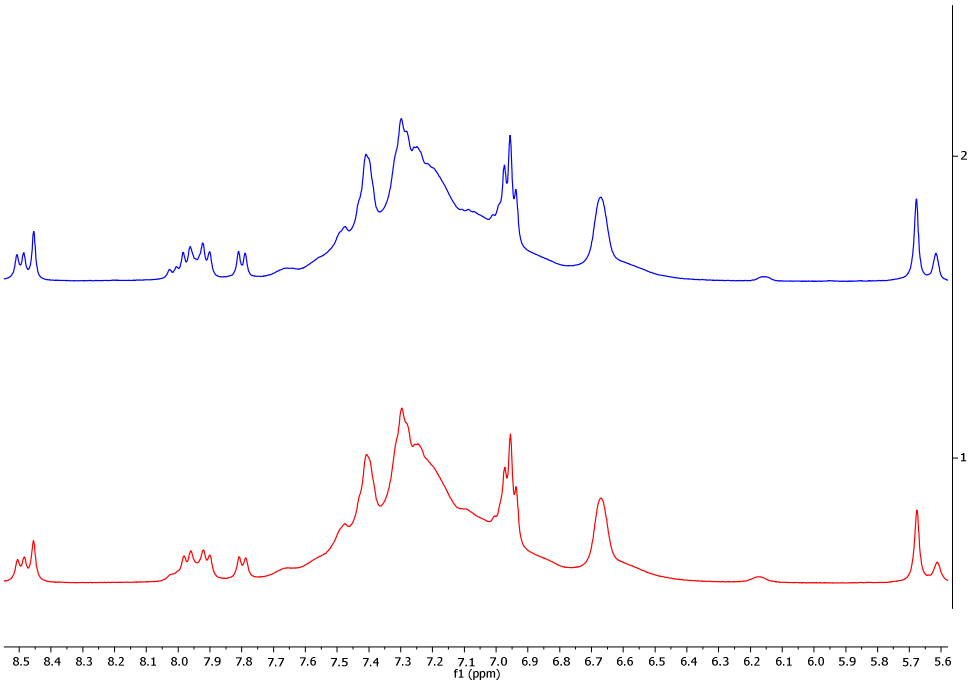

Figure S11. Stability test in d3-acetonitrile of **2a**. ^{1}H NMR (300MHz) recorded on the same probe after 1 week.

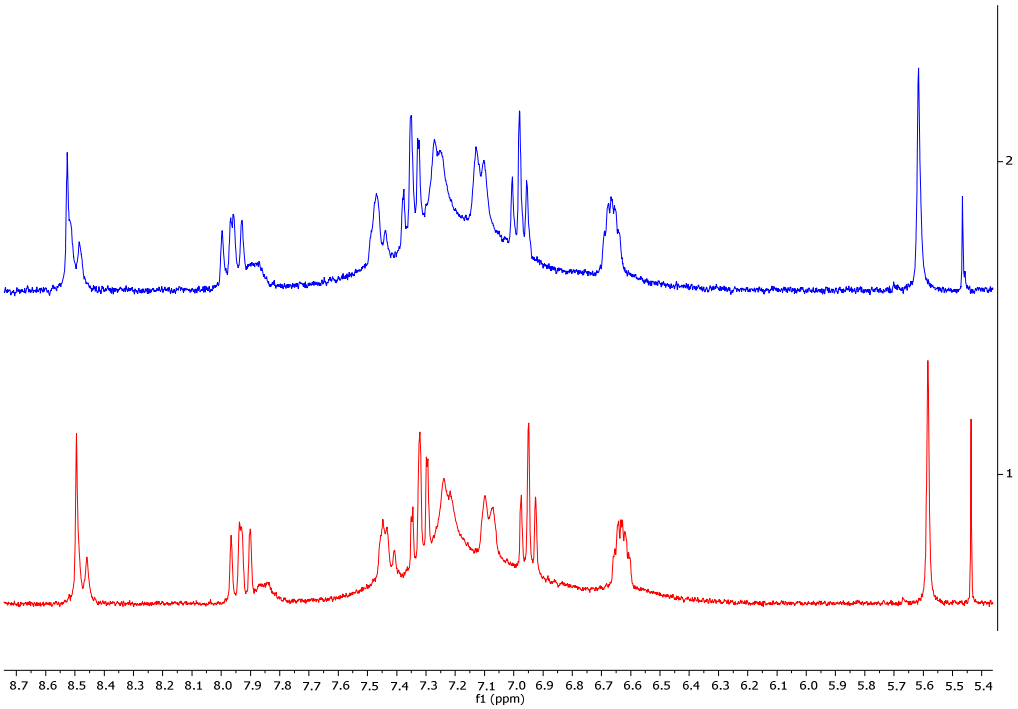

Figure S12. Stability test in d3-acetonitrile of **2b**. ^{1}H NMR (300MHz) recorded on the same probe after almost 3 months (Top, blue spectrum).

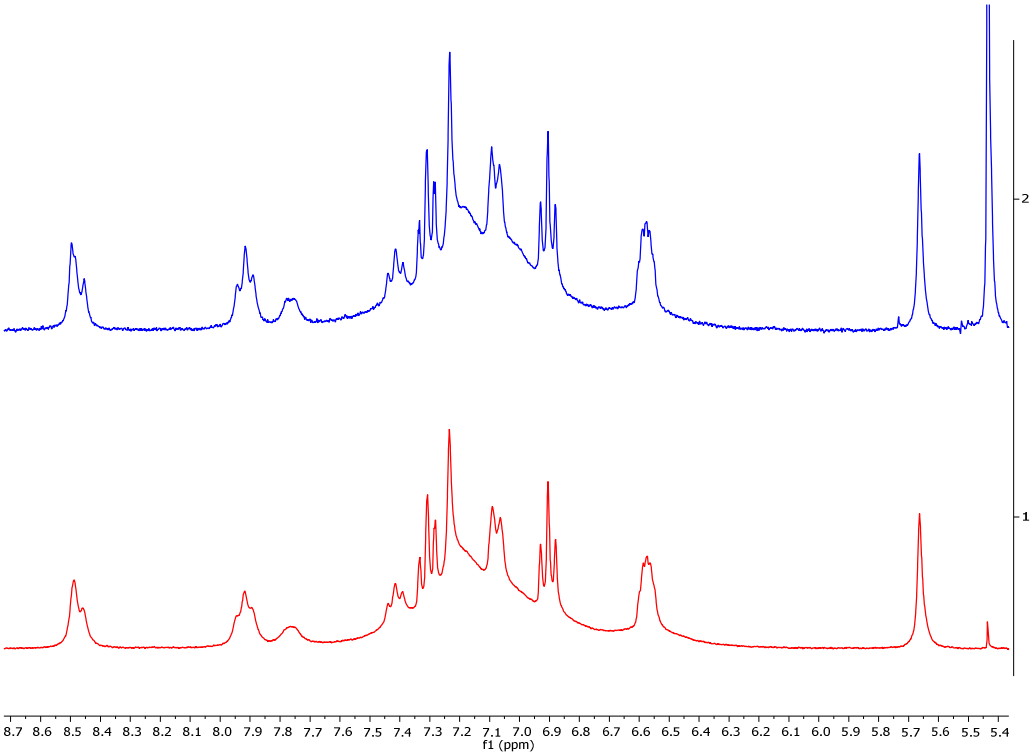

Figure S13. Stability test in d3-acetonitrile of **2c**. ^{1}H NMR (300MHz) recorded on the same probe after almost 3 months (Top, blue spectrum).

3. High-resolution ESI Mass Spectra

These experiments were done with an LTQ Orbitrap XL from Thermo Scientific

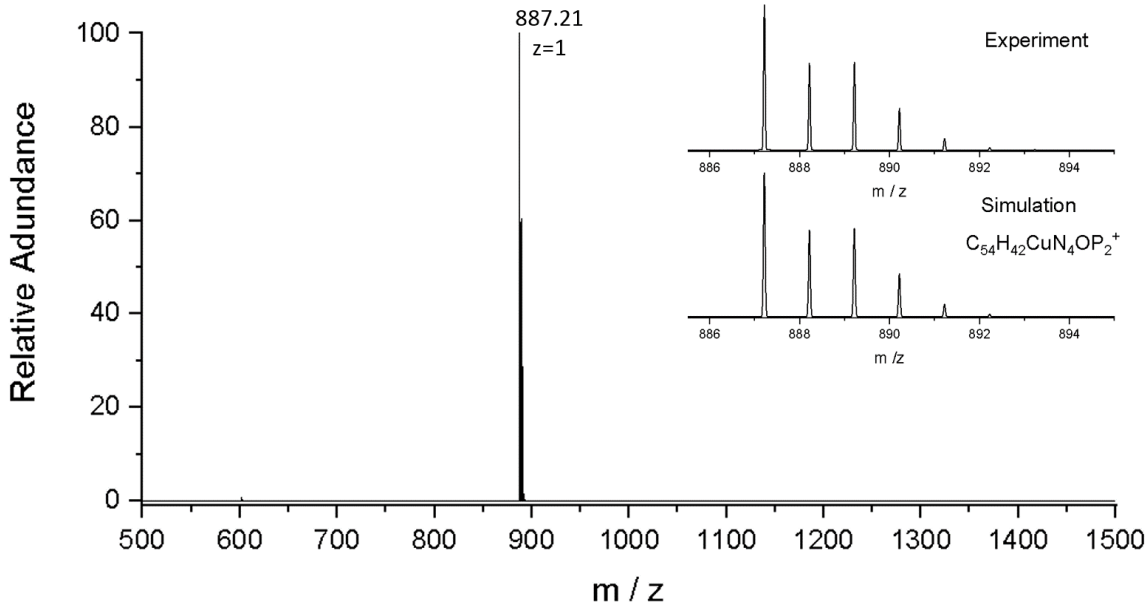

Figure S14. HR-ESI-MS of compound **1**.

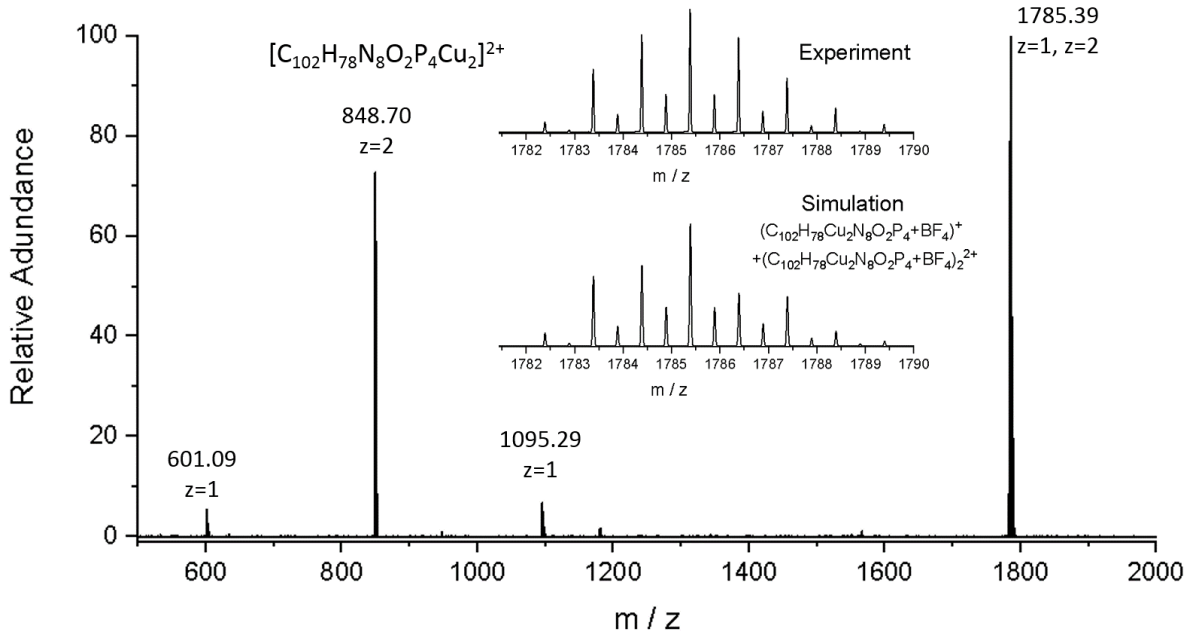

Figure S15. HR-ESI-MS of compound **2a**.

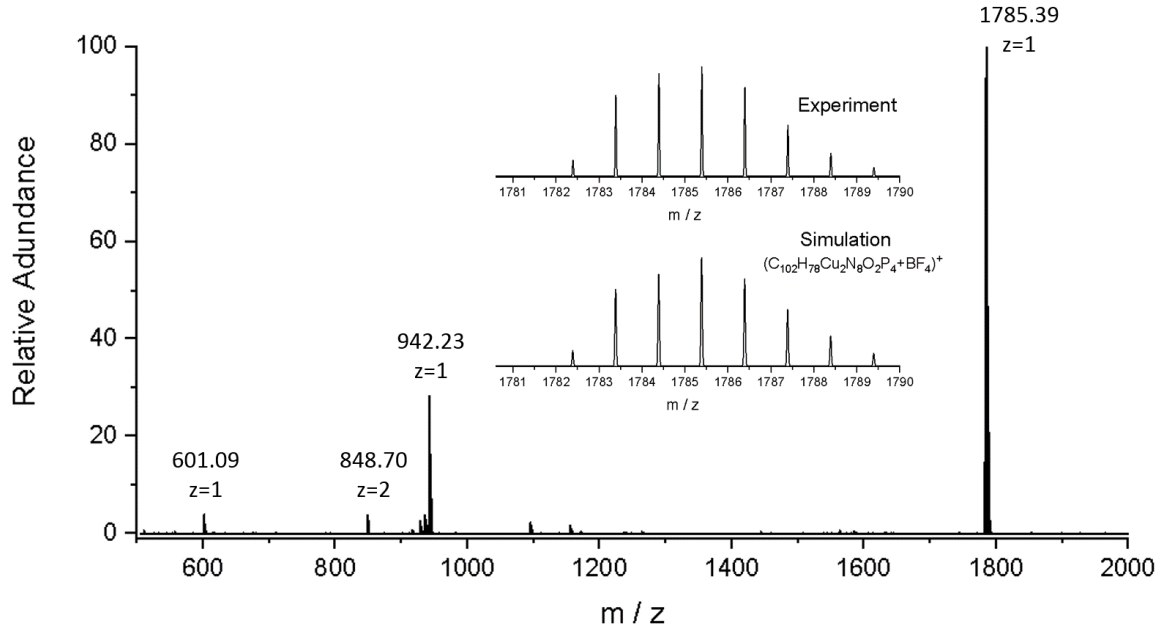

Figure S16. HR-ESI-MS of compound **2b**.

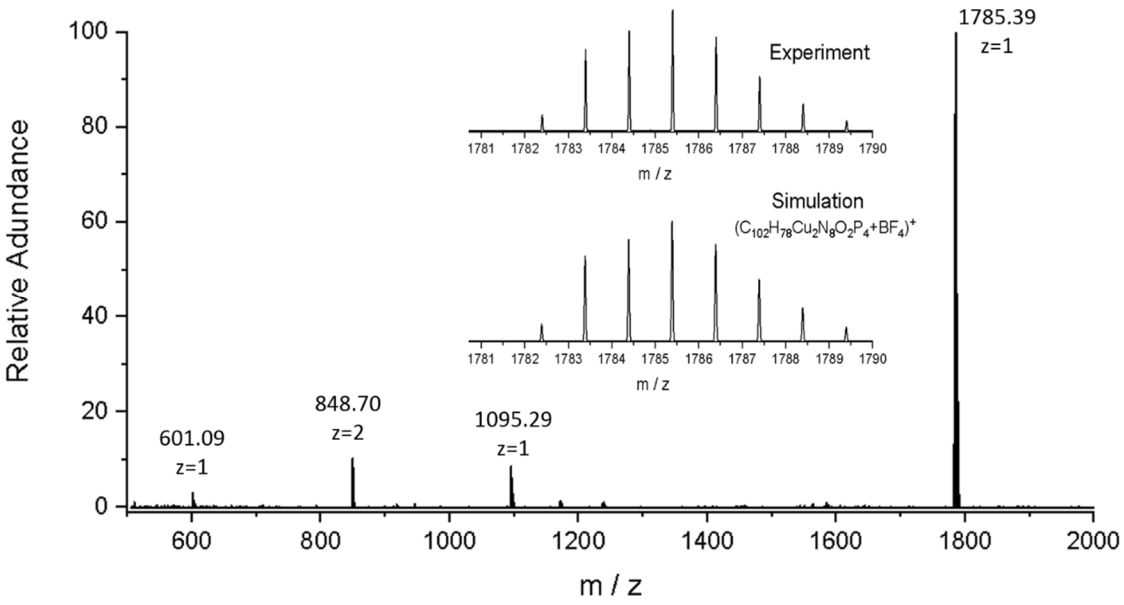

Figure S17. HR-ESI-MS of compound **2c**.

4. Photophysical data in dichloromethane

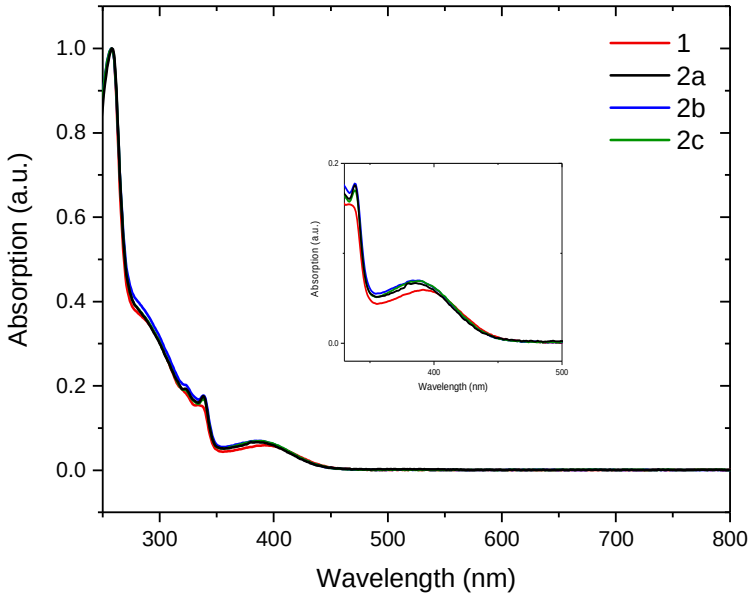

Figure S18. Absorption spectra of compounds **1**, **2a-c** in dichloromethane ([c]≈10^{-5}M). The maximum of the ^{1}MLCT is at 395 nm for **1**, and 388 nm for compounds **2a-c**. Inset: zoom-in in the range of the MLCT.

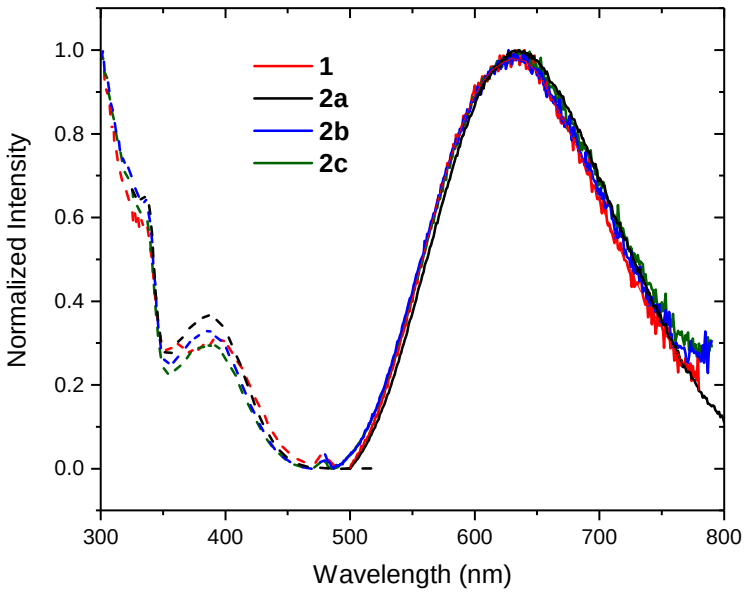

Figure S19. Excitation (dashed plots) and emission (solid plots) spectra of compounds **1**, **2a-c** in dichloromethane ([c]≈10^{-6}M). Emissions were recorded exciting at 415 nm (compounds **1** and **2a**) and at 400 nm for compounds **2b** and **2c**.

5. Photostability in acetonitrile

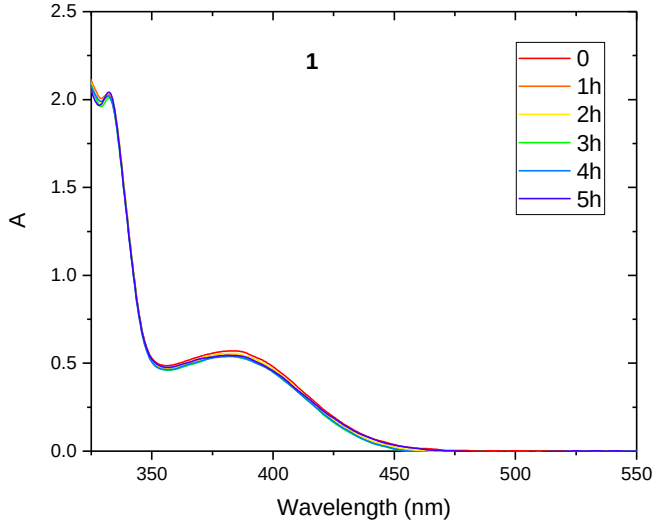

Figure S20. UV-vis absorption of a solution of **1** in acetonitrile after irradiation time at 420 nm.

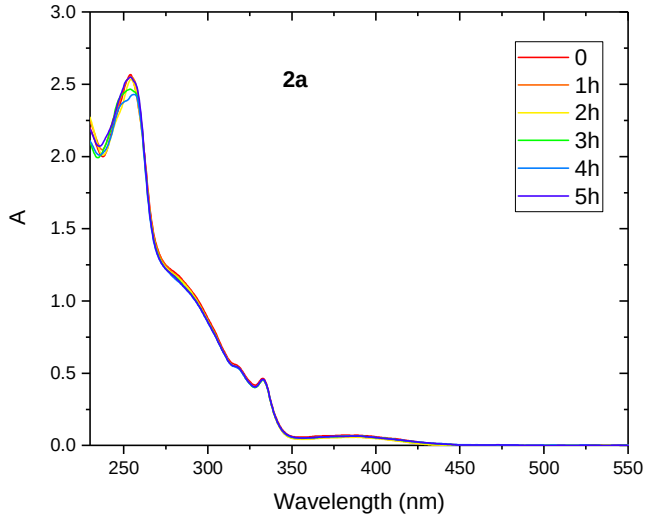

Figure S21. UV-vis absorption of a solution of **2a** in acetonitrile after irradiation time at 420 nm.

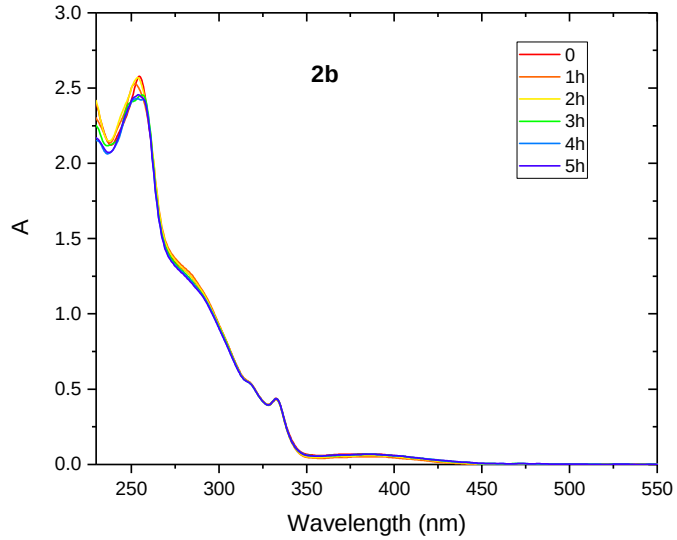

Figure S22. UV-vis absorption of a solution of **2b** in acetonitrile after irradiation time at 420 nm.

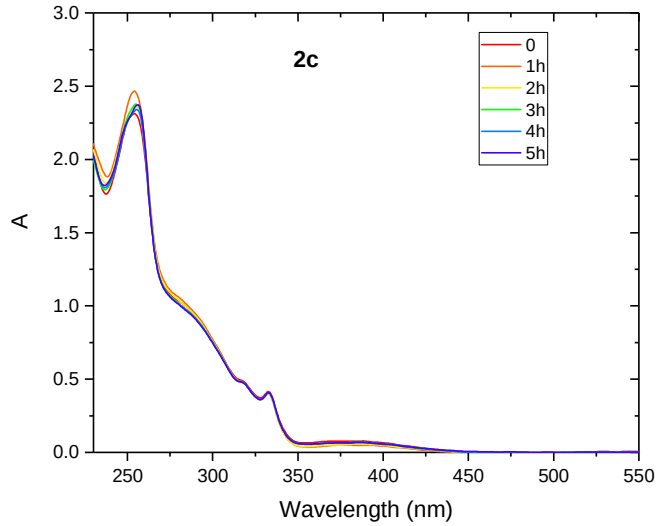

Figure S23. UV-vis absorption of a solution of **2c** in acetonitrile after irradiation time at 420 nm

6. Cyclic Voltammetry

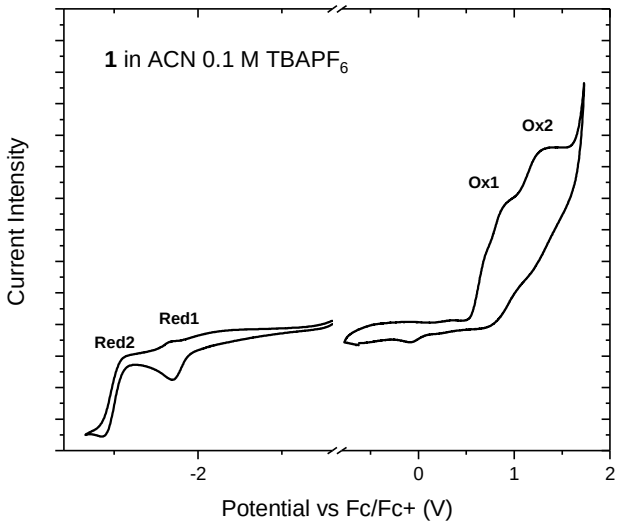

Figure S24. Cyclic voltammetry of complex **1** in acetonitrile (0.1M $TBAPF_6$). Scan rate 100mV/s.

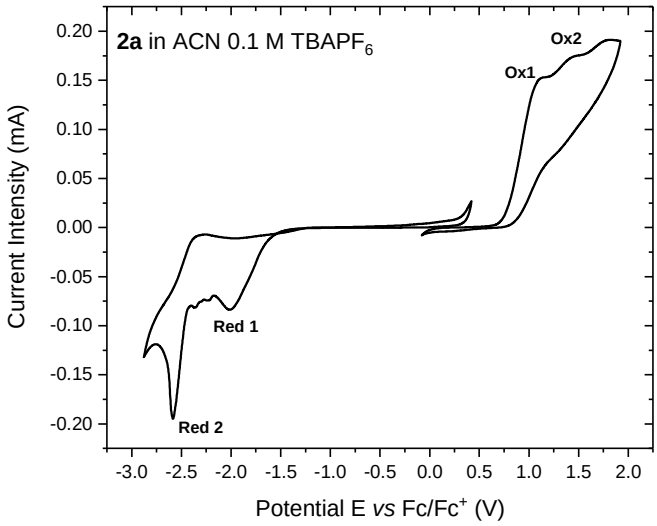

Figure S25. Cyclic voltammetry of complex **2a** in acetonitrile (0.1M $TBAPF_6$). Scan rate 100mV/s.

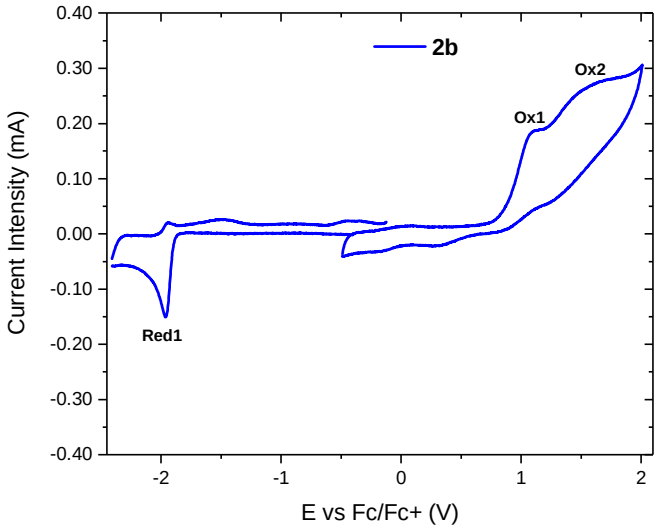

Figure S26. Cyclic voltammetry of complex **2b** in acetonitrile (0.1M $TBAPF_6$). Scan rate 100mV/s.

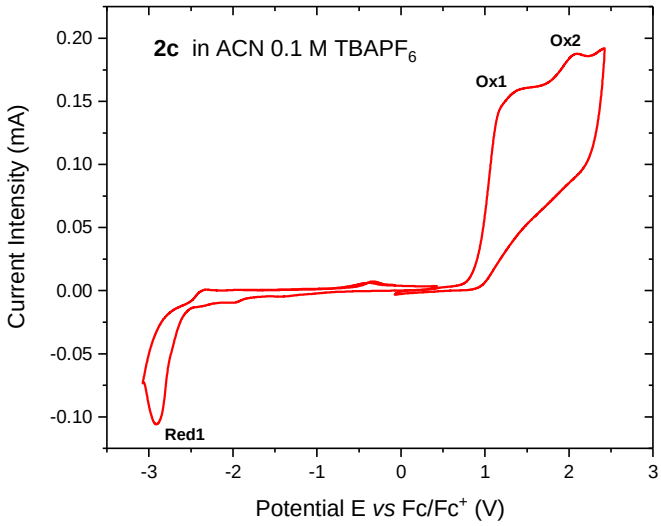

Figure S27. Cyclic voltammetry of complex **2c** in acetonitrile (0.1M $TBAPF_6$). Scan rate 100mV/s.

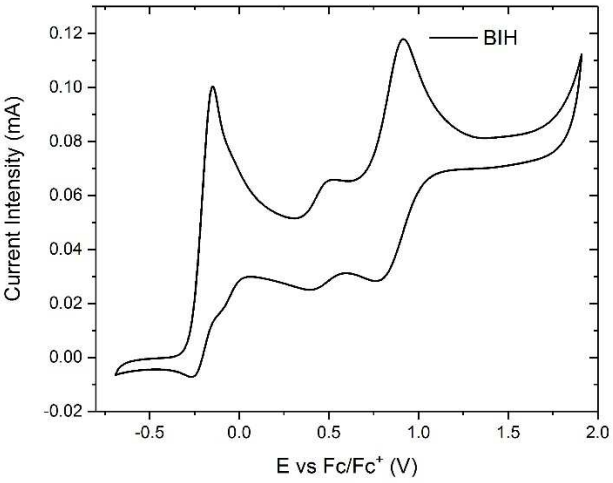

Figure S28. Cyclic voltammetry of sacrificial electron donor BIH in acetonitrile (0.1M $TBAPF_6$). Scan rate 100mV/s. The first oxidation process is at -0.204 V versus Fc/Fc^+ couple.

Table S1. Estimation of the driving force of the reductive quenching between PS and BIH.

PS	E_{ox}*/V	E_{red}*/V	ΔG_{red}
1	-1.75	0.61	-0.81
2a	-1.81	0.85	-1.05
2b	-1.31	0.75	-0.95
2c	-1.71	0.06	-0.26

7. Stern-Volmer bimolecular quenching

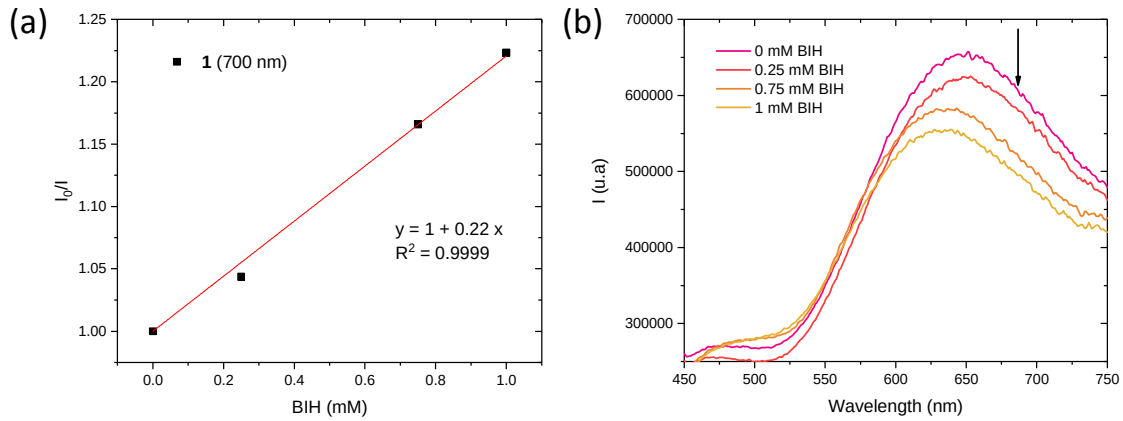

Figure S29. Stern-Volmer quenching studies of 1. (a) linear fit; (b) emission spectra collected recorded with increasing concentration of BIH, excitation at 390 nm.

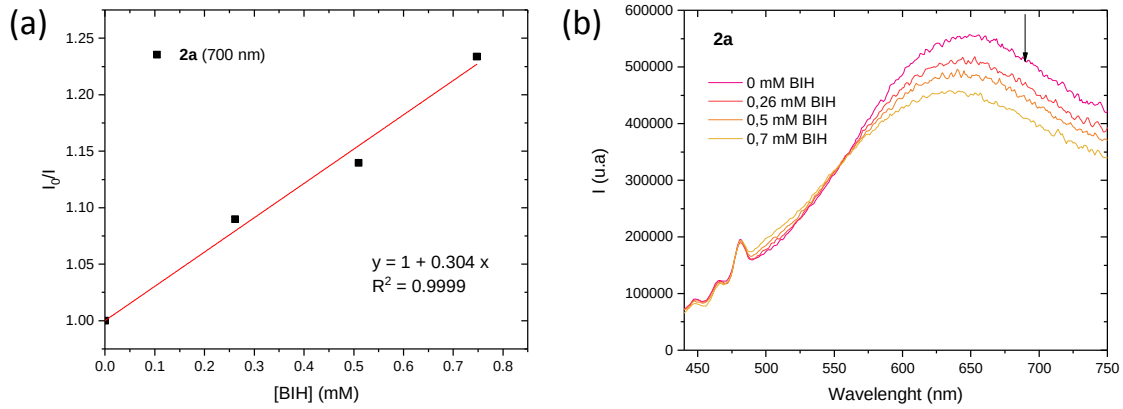

Figure S30. Stern-Volmer quenching studies of **2a**. (a) linear fit; (b) emission spectra collected recorded with increasing concentration of BIH, excitation at 420 nm.

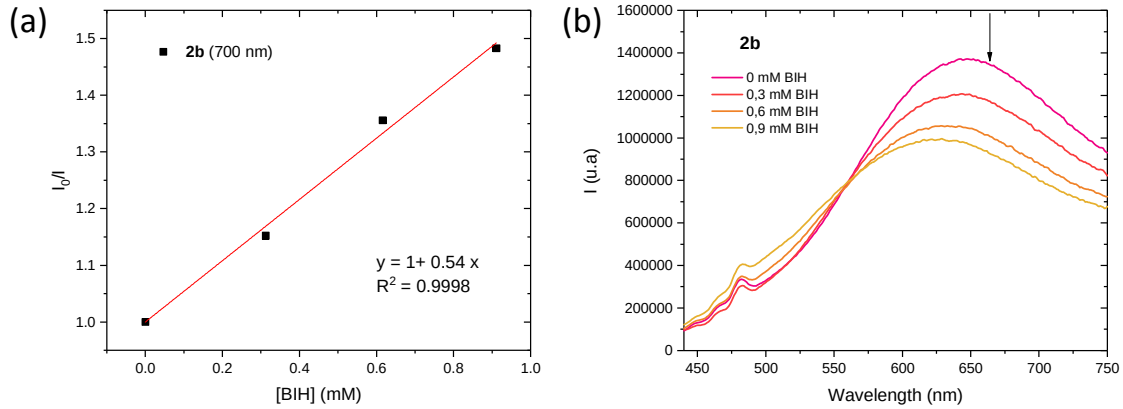

Figure S31. Stern-Volmer quenching studies of **2b** (a) linear fit; (b) emission spectra collected recorded with increasing concentration of BIH, excitation at 420 nm.

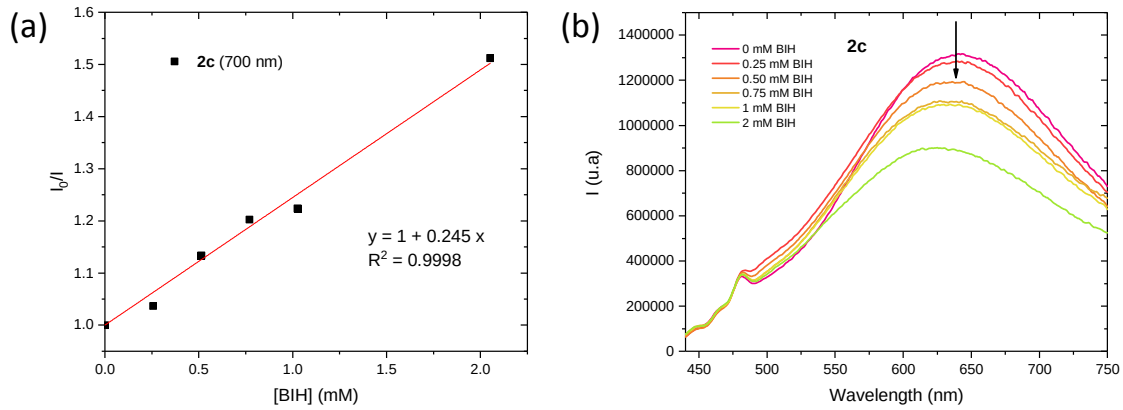

Figure S32. Stern-Volmer quenching studies of **2c**. (a) Fitting ; (b) emission spectra collected recorded with increasing concentration of BIH, excitation at 420 nm.

8. Photoactivated CO_2 reduction

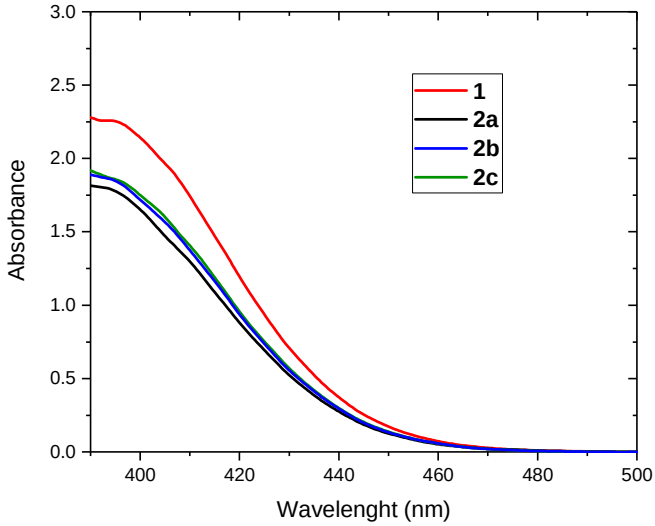

Figure S33. Absorption spectra of the photocatalytic solutions in CH_3CN:TEOA (5:1) containing 20 mM BIH and 0.1mM CAT with the following Cu-PS: **1** (1mM) red line; **2a** (0.5mM) black line; **2b** (0.5 mM) blue line; **2c** (0.5 mM) green line.

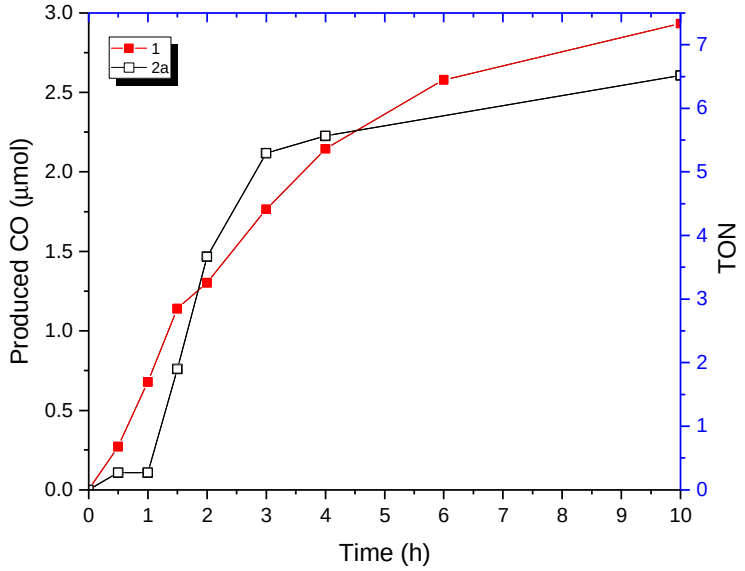

Figure S34. CO evolution and turnover numbers as a function of irradiation time. Reactions were performed with 1mM concentration for **1** and 0.5 mM concentration for **2a**.

9. Crystallographic data for complexes 1, 2a, 2b and 2c

Crystallographic data for compounds **1**, **2a**, **2b** and **2c** reported in this paper have been deposited with the Cambridge Crystallographic Data Centre as supplementary information no. CCDC-1988207–1988210. Copies of the data can be obtained free of charge from https://www.ccdc.cam.ac.uk/structures/.

Experimental Details.

Single crystal X-ray diffraction data were collected on a STADI VARI diffractometer with monochromated Ga Kα (λ = 1.34143 Å) or Mo Kα (λ = 0.71073) radiation at low temperature. Using Olex2 ,[1] the structures were solved with the ShelXT[2] structure solution program using Intrinsic Phasing and refined with the ShelXL[3]refinement package using Least Squares minimization. Refinement was performed with anisotropic temperature factors for all non-hydrogen atoms; hydrogen atoms were calculated on idealized positions.

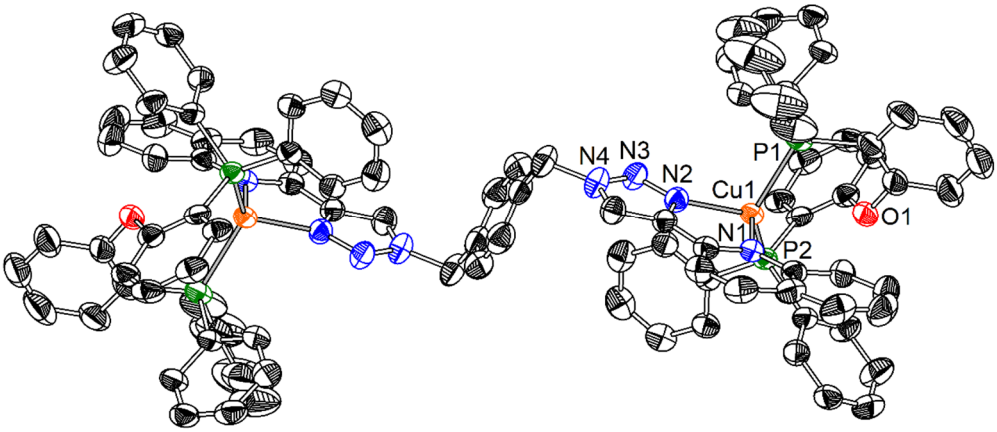

Figure S35. ORTEP structure of complex **2c** shown at the 50% probability level. Hydrogen atoms, counterion and solvent molecules were omitted for clarity.

Table S2. Crystallographic data of **1** and **2a**.

Compound	**1**·1.5(CH_2Cl_2)	**2a**·3(CH_2Cl_2)
Empirical formula	$C_{55.5}H_{45}BCl_3CuF_4N_4OP_2$	$C_{105}H_{84}B_2Cl_6Cu_2F_8N_8O_2P_4$
Formula weight	1102.59	2127.08
Temperature/K	150	180.0
Crystal system	monoclinic	triclinic
Space group	$P2_1/n$	$P1$
a/Å	13.8639(2)	10.3631(3)
b/Å	45.5647(6)	15.4695(4)
c/Å	16.5949(2)	16.8270(4)
α/°	90	96.516(2)
β/°	96.5850(10)	95.136(2)
γ/°	90	97.236(2)
Volume/Å^3	10413.9(2)	2644.01(12)
Z	8	1
ρ_{calc}g/cm^3	1.407	1.336
μ/mm^{-1}	3.879	0.680
F(000)	4520.0	1088.0
Radiation	GaKα (λ = 1.34143)	MoKα (λ = 0.71073)
2Θ range for data collection/°	4.96–127.9	2.45–66.8
Reflections collected	68449	53144
Independent reflections	25109 [R_{int} = 0.0199, R_σ = 0.0282]	30488 [R_{int} = 0.0332, R_σ = 0.0477]
Reflections with I ≥ 2σ(I)	20028	21084
Data/restraints/parameters	25109/0/1288	30488/21/1217
Goodness-of-fit on F^2	1.057	0.988
Final R indexes [I ≥ 2σ(I)]	R_1 = 0.0571, wR_2 = 0.1563	R_1 = 0.0739, wR_2 = 0.2114
Final R indexes [all data]	R_1 = 0.0731, wR_2 = 0.1666	R_1 = 0.1012, wR_2 = 0.2366
Largest diff. peak/hole / e Å^{-3}	1.42/–1.18	1.73/–0.82
Flack parameter		0.263(13)
CCDC number	1988207	1988208

Table S3. Crystallographic data of **2b** and **2c**

Compound	**2b**·$C_4H_8O_2$	**2c**·4(CH_2Cl_2)
Empirical formula	$C_{106}H_{80}B_2Cu_2F_8N_8O_4P_4$	$C_{106}H_{86}B_2Cl_8Cu_2F_8N_8O_2P_4$
Formula weight	1954.36	2212.00
Temperature/K	150.0	150
Crystal system	triclinic	triclinic
Space group	$P\bar{1}$	$P\bar{1}$
a/Å	14.7119(9)	9.5700(7)
b/Å	17.1432(6)	16.7662(15)
c/Å	23.5508(12)	17.2319(11)
α/°	106.731(3)	90.522(6)
β/°	96.377(4)	101.190(6)
γ/°	96.990(4)	105.301(6)
Volume/Å^3	5578.9(5)	2610.9(4)
Z	2	1
ρ_{calc}g/cm^3	1.163	1.407
μ/mm^{-1}	2.745	4.170
F(000)	2008.0	1130.0
Radiation	GaKα (λ = 1.34143)	GaKα (λ = 1.34143)
2Θ range for data collection/°	4.746–100.0	8.512–120.0
Reflections collected	43829	30829
Independent reflections	16651 [R_{int} = 0.1139, R_σ = 0.0855]	11484 [R_{int} = 0.0291, R_σ = 0.0432]
Reflections with I ≥ 2σ(I)	9542	7677
Data/restraints/parameters	16651/0/1207	11484/78/631
Goodness-of-fit on F^2	1.259	1.074
Final R indexes [I ≥ 2σ(I)]	R_1 = 0.1163, wR_2 = 0.3040	R_1 = 0.0901, wR_2 = 0.2680
Final R indexes [all data]	R_1 = 0.1650, wR_2 = 0.3438	R_1 = 0.1220, wR_2 = 0.2877
Largest diff. peak/hole / e Å^{-3}	0.87/–1.34	2.26/–1.18
CCDC number	1988209	1988210

10. Literature comparison

Table S4. Photocatalytic reduction of CO_2 using $[Ni(cyclam)]^{2+}$ as the catalyst

PS	e-D	solvent	TON (CO)	Other info[(a)]	time	Reference
$[Ru(bpy)_3]^{2+}$	ascorbate	H_2O	n.r.	50 µL CO	4 h	[4]
$[Ru(bpy)_3]^{2+}$	ascorbate	H_2O	n.r.	Φ = 0.06%	4 h	[5]
$[Ru(phen)_3]^{2+}$ [(b), (c)]	ascorbate	H_2O	n.r.	0.32 µL CO	4 h	[6]
$[Ru(bpy)_3]^{2+}$[(c)]	ascorbate	H_2O	n.r.	23.6 µL CO	n.r.	[7]
$[Ru(bpy)_3]^{2+}$	ascorbate	H_2O	8.2 [(d)]		1h	[8]
$[Ru(bpy)_3]^{2+}$	ascorbate	H_2O/supercritical CO_2	2.1	--	4h	[9]
$[Ru(bpy)_3]^{2+}$	ascorbate	CH_3CN/H_2O	5.2	--	60 h	[10]
$[Ru(bpy)_3]^{2+}$	ascorbate	H_2O	38[(e)]		5 h	[11]
ZnSe quantum dots	2-(dimethylamino) ethanethiol	DMF[(f)]/H_2O	283[(g)]		20 h	[12]
$[Cu(NN)(PP)]^+$ – **1**-	BIH	CH_3CN/TEOA	4.3	Φ = 1.0%	4 h	**This work**
$[Cu(NN)(PP)]_2^{2+}$ **2a**-	BIH	CH_3CN/TEOA	4.9	Φ = 1.2 %	4 h	**This work**
$[Cu(NN)(PP)]_2^{2+}$ **2b**-	BIH	CH_3CN/TEOA	8.1	Φ = 2.1 %	4 h	**This work**
$[Cu(NN)(PP)]_2^{2+}$ **2c**-	BIH	CH_3CN/TEOA	4.6	Φ = 1.1 %	4 h	**This work**

(a)Other information regarding the amount of produced CO when TON values are missing; (b) phen = phenanthroline; (c) $[Ni(cyclam)]^{2+}$ is covalently attached to PS, (d) with bimacrocyclic catalyst $[Ni(cyclam)]_2^{4+}$; (e)$[Ni(cyclam)]^{2+}$ is incorporated in Cu-azurin; (f) DMF= *N,N*-dimethylformamide; (g) with heterogeneous photosensitizer.

11. References

[1] O. V. Dolomanov, L. J. Bourhis, R. J. Gildea, J. A. K. Howard, H. Puschmann, *Journal of Applied Crystallography* **2009**, *42*, 339-341.

[2] G. Sheldrick, *Acta Crystallographica Section A* **2015**, *71*, 3-8.

[3] G. Sheldrick, *Acta Crystallographica Section C* **2015**, *71*, 3-8.

[4] J. L. Grant, K. Goswami, L. O. Spreer, J. W. Otvos, M. Calvin, *Journal of the Chemical Society, Dalton Transactions* **1987**, 2105-2109.

[5] C. A. Craig, L. O. Spreer, J. W. Otvos, M. Calvin, *The Journal of Physical Chemistry* **1990**, *94*, 7957-7960.

[6] E. Kimura, X. Bu, M. Shionoya, S. Wada, S. Maruyama, *Inorg. Chem.* **1992,**, *31*, 4542-4546.

[7] E. Kimura, S. Wada, M. Shionoya, Y. Okazaki, *Inorg. Chem.* **1994**, *33*, 770-778.

[8] K. Mochizuki, S. Manaka, I. Takeda, T. Kondo, *Inorganic Chemistry* **1996**, *35*, 5132-5136.

[9] M. A. Méndez, P. Voyame, H. H. Girault, *Angewandte Chemie International Edition* **2011**, *50*, 7391-7394.

[10] C. Herrero, A. Quaranta, S. El Ghachtouli, B. Vauzeilles, W. Leibl, A. Aukauloo, *Physical Chemistry Chemical Physics* **2014**, *16*, 12067-12072.

[11] C. R. Schneider, H. S. Shafaat, *Chemical Communications* **2016**, *52*, 9889-9892.

[12] M. F. Kuehnel, C. D. Sahm, G. Neri, J. R. Lee, Katherine L. Orchard, A. J. Cowan, E. Reisner, *Chemical Science* **2018**, *9*, 2501-2509.